Available online at www.sciencedirect.com
ScienceDirect
Trans. Nonferrous Met. Soc. China 29(2019) 2392−2399
Transactions of Nonferrous Metals Society of China
www.tnmsc.cn

Implicit modeling of complex orebody with constraints of geological rules

De-yun ZHONG, Li-guan WANG, Lin BI, Ming-tao JIA

School of Resources and Safety Engineering, Central South University, Changsha 410083, China

Received 19 September 2018; accepted 27 August 2019

Abstract: To dynamically update the shape of orebody according to the knowledge of a structural geologist's insight, an approach of orebody implicit modeling from raw drillhole data using the generalized radial basis function interpolant was presented. A variety of constraint rules, including geology trend line, geology constraint line, geology trend surface, geology constraint surface and anisotropy, which can be converted into interpolation constraints, were developed to dynamically control the geology trends. Combined with the interactive tools of constraint rules, this method can avoid the shortcomings of the explicit modeling method based on the contour stitching, such as poor model quality, and is difficult to update dynamically, and simplify the modeling process of orebody. The results of numerical experiments show that the 3D ore body model can be reconstructed quickly, accurately and dynamically by the implicit modeling method.

Key words: three-dimensional geomodeling; implicit modeling; radial basis function; structural anisotropy; geological rules

1 Introduction

Due to the limitation of geological conditions and exploration technology, complete and regular geological data cannot be obtained in geological exploration, and there is great uncertainty in modeling sparse data. The method of interpreting and 3D modeling of the complex orebody by artificial experience and human-computer interaction is inefficient, arbitrary and subjective, and difficult to update the orebody model. Therefore, it is of great significance to dynamically reconstruct the three-dimensional orebody models close to the original shape from the raw data and geological interpretation of multi-source and sparse sampling.

The methods of geology modeling can be divided into two kinds, termed explicit modeling and implicit modeling [1]. The geometrical quality of the model built by the traditional explicit modeling method is not high enough, and there are a lot of degenerate triangles, which are prone to reveal defects such as opening and self-intersection. Implicit modeling recovers the three-dimensional orebody model through surface reconstruction using an implicit function. Compared with the traditional explicit modeling method, the implicit modeling method has the advantages of high mesh quality, repeatable process, global uncertainty and dynamic updating [2−4].

In the past two decades, a variety of implicit function interpolation methods including the discrete smooth interpolation (DSI) method [5], the (radial basis function, RBF) RBF-based method [6,7], the Hermite RBF (HRBF) method [8] and the moving least squares (MLS) method [9] have been developed. These methods are mainly applied to dense point cloud data of three-dimensional laser scanning and are difficult to fit sparse and uneven sampling data of geological exploration with various geological rules and constraints. Among them, RBF is a widely used interpolation method with complete theoretical support, which has been integrated into Leapfrog Geo software [10] and widely used in geological modeling. CARR et al [11] solved the problem of fast interpolation of large-scale point cloud data by introducing the fast multipole method (FMM). And the Leapfrog Geo software uses the similar method, FastRBF method [12,13], to interpolate large geological data sets efficiently. JONES and CHEN [14] transformed the contours into the three-dimensional distance field using the distance transformation by the contours of the orebody and reconstructed the model by iso-surface extraction. GUO et al [15] conducted a preliminary study on geological interfaces modeling using HRBF method with section constraints.

The traditional RBF methods are based on domain

Corresponding author: Lin BI; Tel: +86-731-88877665; E-mail: mr.bilin@163.com
DOI: 10.1016/S1003-6326(19)65145-9

constrains, which are difficult to handle complex geological structural trends. More and more attention has been paid to the study of the RBF-based methods with generalized constraints recently. Several extended interpolants based on the theory of Hermite−Birkhoff interpolation with radial basis functions are developed to interpolate anisotropic and first-order Hermite data (points with normals), such as anisotropic RBF (ARBF) [16,17], generalized RBF (GRBF) [18] and generalized HRBF (GHRBF) [19,20]. More recently, a generalized interpolation framework using RBF from scattered multivariate structural data was presented by HILLIER et al [18] to generate continuous geological surfaces. However, each interpolation method has its own advantages and drawbacks, and is applicable to specific conditions. It is necessary to study interpolation methods that meet the constraints of specific geological rules in different situations to ensure the accuracy of geological model.

The implicit modeling method is based on the reconstruction of an implicit function from the drillhole datasets. The geology space constructed by the combination of drilling samples is transformed into a signed distance field. The result of complex orebody model is expressed as a mathematical function, and the implicit surface is represented as a zero-level set of the function. To consider various types of geological rules, the GRBF interpolant was used as the implicit function. One of the advantages of this approach is that it can generate geometrically valid 3D ore body models directly from the raw drillhole data with or without the constraints of interpretation.

2 Mathematical framework

The GRBF interpolant is built upon the theory of generalized Hermite−Birkhoff interpolation [18−22] with radial basis functions. We will first review the relevant theory loosely.

Given the known data $(\boldsymbol{x}_i, \lambda_i f)$, $i=1, 2, \cdots, N$, $\boldsymbol{x}_i \in \mathbf{R}^n$, where λ_i is a linearly independent set of continuous linear functionals and f is some (smooth) data function, the generalized Hermite interpolation problem tries to construct the interpolant $s(\boldsymbol{x})$ satisfying $\lambda_i s(\boldsymbol{x})=\lambda_i f$ as

$$s(\boldsymbol{x})=\sum_{j=1}^{N}\omega_j\lambda_j^{\boldsymbol{x}'}\Phi(\boldsymbol{x},\ \boldsymbol{x}')+p(\boldsymbol{x}),\ s\in H \tag{1}$$

where $\lambda_j^{\boldsymbol{x}'}$ is continuous linear functional acting on a usual radial basis function $\Phi(\boldsymbol{x}, \boldsymbol{x}')$ viewed as a function of $\boldsymbol{x}'=(x', y', z')$. When conditionally positive definite functions are used, it is often required to construct low-order polynomials $p(\boldsymbol{x})$ to ensure that the function converges.

Four types of general constraints [18−22] can be constructed by the different operations of the continuous linear functional and the distance transformation, as shown in Fig. 1.

(1) Domain constraints: The domain constraints are locations at which we require the implicit function to take on the specific values. The given μ scattered data points $\{\boldsymbol{x}_i,\ f(\boldsymbol{x}_i)\}_{i=1}^{\mu}$ satisfy

$$f(\boldsymbol{x}_i)=f_i,\ i=1, 2, \cdots, \mu \tag{2}$$

where f_i is the function value of the geological domain.

The domain constraint can well control the internal and external relations of the geological domain and is the most basic constraint to define the geological interface. According to the value of the function, the domain constraints can be divided into three different types: on-surface constraints ($f(\boldsymbol{x}_i)=0$), interior constraints ($f(\boldsymbol{x}_i)<0$) and exterior constraints ($f(\boldsymbol{x}_i)>0$).

(2) Gradient constraints: The gradient constraints refer to the evaluation of some derivative at specific locations. The given σ scattered data points $\{\boldsymbol{x}_i, \nabla f(\boldsymbol{x}_i)\}_{i=\mu+1}^{\mu+\sigma}$ satisfy

$$\nabla f(\boldsymbol{x}_i)=\boldsymbol{n}_i,\ i=\mu+1, \mu+2, \cdots, \mu+\sigma \tag{3}$$

where $\boldsymbol{n}_i$ is the unit normal vector of the geological domain.

The sign of the gradient constraint represents different shape constraints. The normal direction of $\boldsymbol{n}_i$ points to the exterior of the shape, then the opposite direction points to the interior of the shape. The normal constraints can be used to construct the trend surface constraint in the domain.

(3) Tangent constraints: The tangent constraints refer to the sampling orientations tangent to the domain at specific locations. The given τ scattered data points $\{\boldsymbol{x}_i, \langle\nabla f(\boldsymbol{x}_i),\ \boldsymbol{t}_i\rangle\}_{i=\mu+\sigma1}^{\mu+\sigma+\tau}$ satisfy

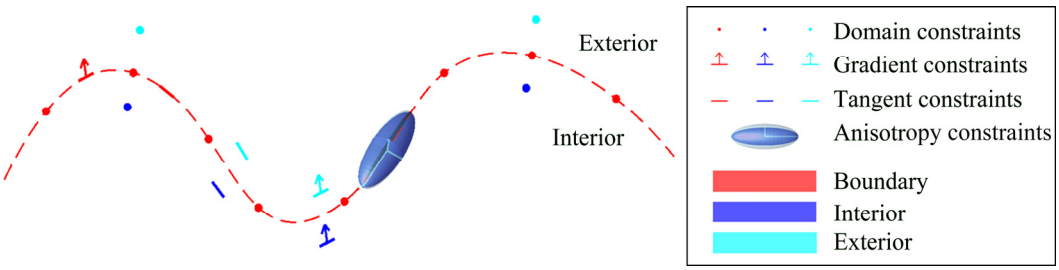

Fig. 1 Various types of interpolation constraints used for implicit modeling

$$\langle \nabla f(\boldsymbol{x}_i),\ \boldsymbol{t}_i \rangle = 0,\ i=\mu+\sigma+1, \mu+\sigma+2,\ \cdots, \mu+\sigma+\tau \quad (4)$$

where $\boldsymbol{t}_i$ is the unit tangent vector of the geological domain.

The tangent constraint does not have the polarity of the orientation, but only affects the direction of adjacent points and changes the local curvature, so it is well suited for constructing trend line constraints in the domain.

(4) Anisotropy constraints: The anisotropy constraints refer to the evaluation of the anisotropy distance by the distance transformation at specific locations. The given N scattered data points $\{\boldsymbol{x}_i,\ \lambda_i f\}_{i=1}^{N}$ satisfy

$$\Phi_{\boldsymbol{T}}(\boldsymbol{x},\ \boldsymbol{x}') = \Phi(\|\boldsymbol{x}-\boldsymbol{x}'\|_{\boldsymbol{T}}) \quad (5)$$

where

$$\|\boldsymbol{x}-\boldsymbol{x}'\|_{\boldsymbol{T}} = \|(\boldsymbol{x}-\boldsymbol{x}')\cdot \boldsymbol{T}\ \| \quad (6)$$

and $\boldsymbol{T}$ is the anisotropic distance matrix which can be constructed via the affine matrix transformation. The anisotropy of its three principal directions represented as an ellipsoid.

The main difference between the isotropic and anisotropic GRBF is the computation of the distance field. Similar to the isotropic GRBF but with a modified distance metric by a distance transformation, the anisotropic general radial basis function (AGRBF) interpolant has the following form:

$$s(\boldsymbol{x}) = \sum_{j=1}^{N} \omega_j' \lambda_j^{x'} \Phi_{\boldsymbol{T}}(\boldsymbol{x},\ \boldsymbol{x}') + p(\boldsymbol{x}),\ s \in H,\ \ N=\mu+\sigma+\tau \quad (7)$$

where the new set of weights ω_j' are different from ω_j computed from the isotropic GRBF interpolant.

The interpolation equation can be obtained by acting the continuous linear functions on the radial basis function. Similarly, the anisotropic interpolation equation can be obtained by acting $\lambda_j^{x'}$ on anisotropic kernel $\Phi_{\boldsymbol{T}}(\boldsymbol{x},\ \boldsymbol{x}')$. Similar to the RBF interpolant, using the anisotropic GRBF interpolant $s(\boldsymbol{x})$ and the general constraints, the unknown weight coefficients can be determined by solving a linear system such as $\boldsymbol{Ax}=\boldsymbol{b}$.

3 Implicit modeling

3.1 Discrete drillhole

To construct the spatial interpolation conditions of an implicit function, it is necessary to discretize the drillhole data sampled from geological exploration. The discretization of drillhole data refers to the process of obtaining the sampling points of sample segments and non-sample segments based on the grade combination of drillhole data. The geological domain containing the whole drillholes is viewed as a non-Euclidean distance field. The sampling points of sample segments and non-sample segments can be transformed into on-surface constraints and off-surface constraints. Then, the implicit function can be formed by interpolating these constraints and solving the corresponding linear system.

During discretization, the distance values of sampling points are initially computed via the distance along the direction of the drilling trajectory. The on-surface constraints are constructed at the two endpoints of the sample segments. The off-surface constraints (including the exterior and interior constraints) are constructed in the sample and non-sample segments. Along the drilling track, the sample segments are sampled discretely from both ends to the middle to construct the interior constraints according to a given sampling interval. The initial function values of the interior constraints are computed according to the sample distance to the nearest on-surface points. To ensure the reliability of the solution, at least one sample point should be sampled in the sample segments. Similarly, the non-sample segments are sampled discretely from both ends to the middle to construct the exterior constraints according to a given sampling interval. The initial function values of the exterior constraints are computed according to the non-sample distance to the nearest on-surface points. As an example of discretization in Fig. 2, the on-surface constraints with zero values are red, the off-surface point constraints with positive values are cyan and the off-surface point constraints with negative values are blue. After the discretization of drillhole data, the on-surface and the off-surface constraints are added to the interpolation equation to solve the implicit function of the orebody model.

3.2 Distance field correction

During the construction of the implicit model, a signed distance field should be formed in the process of distance computation, and the implicit function can be regarded as a signed distance field function. Therefore, the process of orebody implicit modeling can be regarded as the process of constructing a signed distance field in line with the trend of the geological domain using sampling points.

To distinguish the internal and external field of the orebody model, the relationship between the implicit function value and the implicit surface can be expressed as

$$\begin{cases} \boldsymbol{x} \mid f(\boldsymbol{x}) = 0,\ \boldsymbol{x} \in \mathbf{R}^3,\ \text{on the surface} \\ \boldsymbol{x} \mid f(\boldsymbol{x}) = +\text{dist}(\boldsymbol{x},\ \boldsymbol{x}') > 0,\ \boldsymbol{x} \in \mathbf{R}^3, \\ \quad \text{exterior of the surface} \\ \boldsymbol{x} \mid f(\boldsymbol{x}) = -\text{dist}(\boldsymbol{x},\ \boldsymbol{x}') < 0,\ \boldsymbol{x} \in \mathbf{R}^3, \\ \quad \text{interior of the surface} \end{cases} \quad (8)$$

where $\boldsymbol{x}=(x, y, z)$ is a three-dimensional sampling point, and $\text{dist}(\boldsymbol{x}, \boldsymbol{x}')$ is the nearest distance from $\boldsymbol{x}$ to the closest point $\boldsymbol{x}'$ on the surface. As shown in Fig. 3, the colors

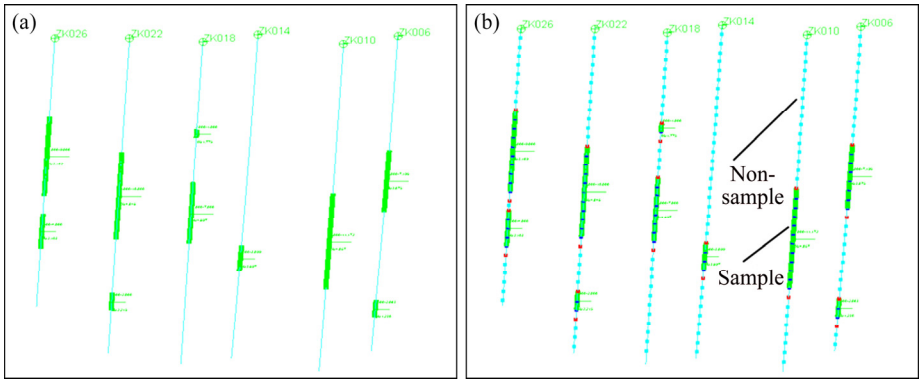

Fig. 2 Discretization procedure of drillholes: (a) Grade combination; (b) Sampling point

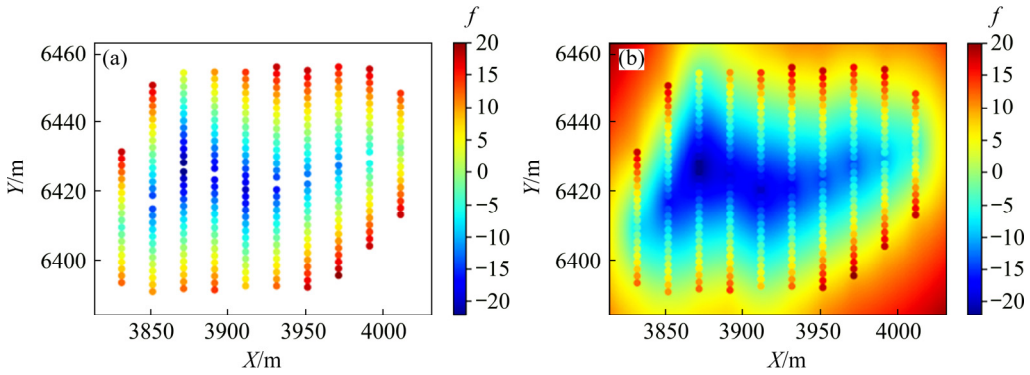

Fig. 3 Signed distance field of drillholes: (a) Discretized points of drillholes; (b) Signed distance field

show different field values, for which blue denotes the maximum negative value and red represents the maximum positive value.

To construct a geological distance more consistent with the trend distribution of the drilling trajectory, the distance values of two points are computed as the length of the drilling trajectory instead of the Euclidean distance. In the process of discrete sampling, the cross-distributed drillholes tend to generate ambiguity constraints with abnormal values, so the distance should be modified according to the distribution of mineralization field. To verify the distance of sampling points, an iterative closest point correction (ICPC) algorithm [23] is used to correct the distance, which ensures the distance field of the implicit function complying with the distribution characteristics of the mineralization field.

4 Constraint with trend

4.1 Constraint rule

The method of implicit modeling still requires the guidance from the structural geologists' expert knowledge, including the designation of multiple geological constraints. Based on the general constraints of the GRBF interpolant, four types of constraint rules can be obtained, as shown in Fig. 4.

(1) Geology trend line

The geology trend line can be used as an orientation constraint to guide the model extension trend of nearby domains. Taking the direction of the trend line as the tangential direction, the trend line is sampled at a certain sampling interval to construct tangent constraints. By specifying trend lines in sparse regions, the reconstructed model has a tendency to extend along the trend line.

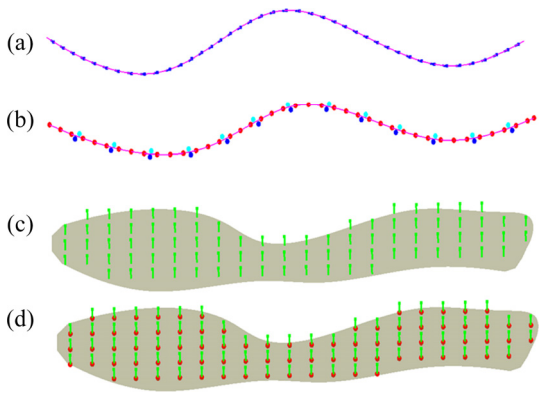

Fig. 4 Four types of constraint rules constructed by general constraints: (a) Geology trend line; (b) Geology constraint line; (c) Geology trend surface; (d) Geology constraint surface

(2) Geology constraint line

The geology constraint line is discretized according to the specified sampling interval, and the discrete constraint points are added to the interpolation equation.

By reconstructing the implicit surface, the orebody model can satisfy the model boundary represented by the constraint line. The geological constraint line can well control the extrapolation boundary of the automatic interpolation model and change the local continuity trend of the model according to the geological rules.

(3) Geology trend surface

The geology trend surface is constructed by the direction sampling (e.g., gradient constraints), but the constraints with specific distance values (e.g., domain constraints) are not constructed. The stratified resampling method is used to resample the trend surface, which can control the uniformity of the resample placement and the minimum distance between samples.

(4) Geology constraint surface

The geology constraint surface represents a local surface modeled by other methods, which can be used to recover the local implicit surface at the sparse locations with incomplete sampling. There are several ways that the constraint surface can be converted to general constraints. One of the ways is to construct both gradient constraints and domain constraints at the sampling points.

4.2 Section constraints

To convert the additional section constraints interpreted by structural geologists into the GRBF interpolation constraints, the contours should be discretized to form domain constraints. To ensure the unique solution of the interpolation equation, the contours of the interpreted sections should be preprocessed to avoid abnormal normal constraints or contradictory domain constraints. Firstly, the redundant points in given tolerance should be removed, and the abnormal segments in the angle tolerance of refraction should be cleared. Secondly, in a certain tolerance range, the sections are preprocessed to reduce the curvature of contours, to build a smoother implicit model. Lastly, the normals of the section will be estimated to construct gradient constrains or off-surface constraints. The off-surface constrains are formed by offsetting the contour points along their normal direction [11]. If the cutting plane of the section orthogonally intersects with the local surface of the orebody model, the normal vector of the boundary surface at $\boldsymbol{p}_i$ can be computed as

$$\boldsymbol{n}_{\boldsymbol{p}_i} = \mathrm{Sign}\boldsymbol{n}_{\boldsymbol{p}_i} \times \frac{\boldsymbol{t}_{\boldsymbol{p}_i} \times \boldsymbol{c}_{\boldsymbol{p}_i}}{\| \boldsymbol{t}_{\boldsymbol{p}_i} \times \boldsymbol{c}_{\boldsymbol{p}_i} \|} \tag{9}$$

where $\boldsymbol{t}_{\boldsymbol{p}_i}$ is the tangent vector of the contour at $\boldsymbol{p}_i$, $\boldsymbol{c}_{\boldsymbol{p}_i}$ is the normal vector of the cutting plane, and $\mathrm{Sign}\boldsymbol{n}_{\boldsymbol{p}_i}$ is the sign of the normal vector determined by the side of the contour. For other cases, the normals of sections are estimated via the method proposed by HECKEL et al [24]. Moreover, the user is allowed to interactively add, remove or edit the local normals at discrete points. Then, the unknown normals can be automatically interpolated by the given ones.

The additional section constraints can be used to guide the topological connection between drilling holes and form the orebody model to satisfy the mineralization trend, as shown in Fig. 5. There are many section constraints shown as green polylines in Fig. 5(a) and geology constraint lines shown as red polylines in Fig. 5(c).

5 Fast modeling

The implicit modeling based on GRBF can be finally transformed into the solution of the linear system $\boldsymbol{Ax}=\boldsymbol{b}$. It consists of two processes, spatial interpolation of an implicit function based on interpolation constraints and three-dimensional surface reconstruction based on point evaluations. To ensure the rapid dynamic updating of the implicit model, in addition to the fast solution of the interpolation equation, the implementation of the fast evaluation of implicit function is also required.

To improve the speed of solving large-scale linear equations, an iterative method, GMRES, proposed by SAAD and SCHULTZ [25], is recommended for implementation. This method belongs to Krylov subspace iteration, which uses Arnoldi iteration to solve the minimum residuals in the subspace to approximate

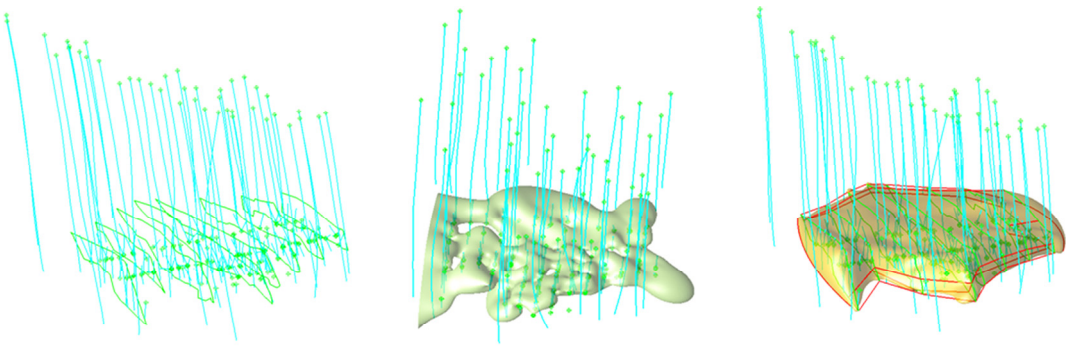

(a) (b) (c)

Fig. 5 Implicit modeling from raw drillhole data: (a) Drillholes and geology constraints; (b) Result without manual constraints; (c) Result with manual constraints

the solution of the linear system. For the problem of complex orebody modeling, it is a very effective method to solve large asymmetric linear equations, which can greatly improve the speed of solving large-scale interpolation equations.

The Marching Cubes method is often used for surface reconstruction. The Marching Cubes algorithm has some ambiguities when extracting the triangular facets of the cubes in the spatial regular data field. To resolve the ambiguity, the hyperbolic asymptote method proposed by NIELSON and HAMANN [26] was implemented. To make full use of the valid cubes in the evaluation process, the surface- following method based on the Marching Cubes algorithm was implemented. The method constructs the initial voxel seed points near the isosurface, using greedy voxel growth rules to track the isosurface by searching the close cubes. It does not evaluate cubes over the whole volume, which can greatly speed up the process of surface reconstruction.

6 Results

The anisotropic GRBF method was implemented and tested on several non-trivial geological examples. These examples contain series of drillhole datasets in sparse data environments. To validate the performance of this method, the results with the traditional radial basis function without constraints were compared.

For sparse drillhole data with large intervals, the reconstructions without constraints are likely to produce discontinuities. Therefore, the modeling method still requires the knowledge of a structural geologist's insight and this input is made in the form of constraint rules, additional sections, and structural anisotropy. The constraint rules were constructed to constrain the shape of the implicit surface according to the actual geological conditions of the drillhole data and the trend of the mineralization domain. Figure 6(d) shows the orebody modeling results directly based on the drillhole data using the traditional radial basis function. It can automatically model without additional constraints. To make the modeling result more consistent with the extension trend of the orebody, the implicit model can be dynamically modified by adding constraint lines and trend surface constraints (Fig. 6(c)). The results (Fig. 6(e)) of implicit modeling of orebody meet the interpretation requirements of structural geologists.

The ore grade shells, geology interfaces or structural trends will be represented by the implicit functions, which can effectively handle the problems encountered in the traditional explicit modeling. Figure 7 shows the dynamic grade shell models established by

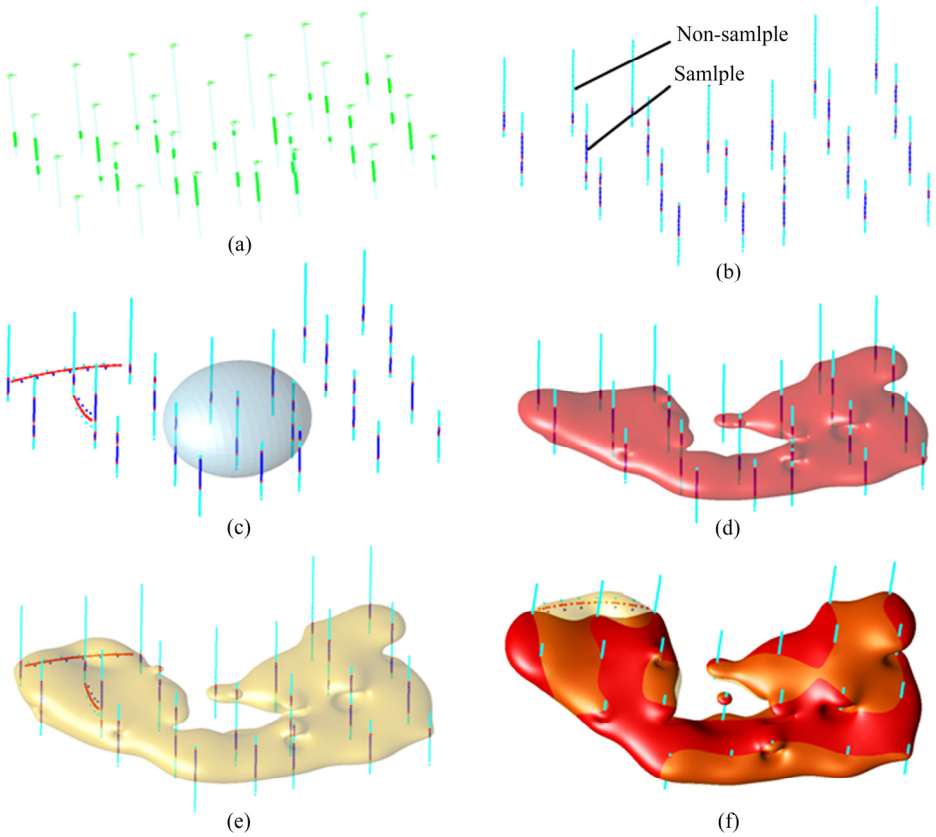

Fig. 6 Processes of implicit modeling from raw drillhole data: (a) Grade combination; (b) Discretization of non-sample and sample segments; (c) User-defined constraint rules; (d) Result without manual constraints; (e) Result with manual constraints; (f) Compared result

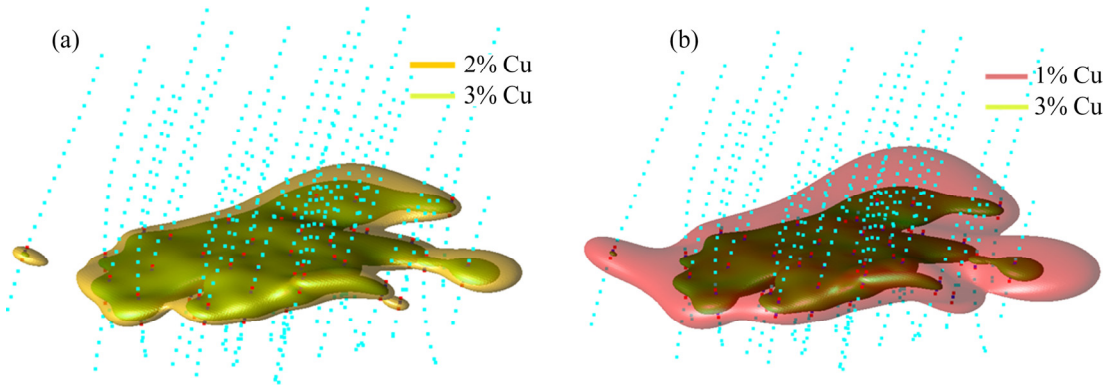

Fig. 7 Dynamic grade shell models with different cut-off grades: (a) 2% and 3%; (b) 1% and 3%

Table 1 Running time of solution and reconstruction of algorithm on several examples

Model	Constraints	Resolution	Triangles	Time/s			
				Solution	MC	PMC	SF
Fig. 6(d)	760	4	17204	1.25	17.87	5.28	1.87
Fig. 6(e)	881	4	17792	2.69	21.83	7.23	2.13
Fig. 7	866	10	38016	2.18	223.52	75.72	4.14

raw drillhole data under different cut-off grades, which can well reflect the spatial distribution trend of the orebody model under different economic indicators. At the same time, the orebody model constructed by implicit modeling has the advantages of high quality and smoothness. It is easy to represent orebody models with complex topology and is convenient to perform Boolean operations.

The performance of the anisotropic GRBF method mainly depends on the number of constraints and the size of resolution. The algorithm was implemented in C++ language and tested on a Windows 64-bit PC with 3.20 GHz Intel(R) Core(TM) i5-3470 and 4GB RAM. Table 1 lists the timings of the solution and reconstruction stages of the algorithm on these examples.

The implementation runs from a few seconds to less than one minute for the examples. The running time is dominated by the solution of large-scale linear systems in the interpolation stage and the evaluation of sampling grids in the reconstruction stage. To test the performance of fast reconstruction using the improved method, the running efficiency of multiple data sets was compared before and after the improvement. Table 1 shows that the surface following (SF) algorithm used has faster reconstruction efficiency than the traditional Marching Cube (MC) and parallel Marching Cube (PMC) extraction method. Moreover, as the size of the solution equations becomes larger or the reconstruction resolution decreases, the performance of the improved algorithm is more obvious.

7 Conclusions

(1) Based on the anisotropic GRBF interpolant, an implicit modeling method of complex orebody conforming to geological rules is proposed, which can convert the geological constraints into different interpolation constraints and constraint rules. It is not based on the grade interpolation but uses the distance field to calculate the implicit function by geological constraints, so that it can be applied to the structural modeling of the orebody. The results show that the reconstructed implicit models are guaranteed to be smooth, continuous and closed geology surface without mistakes such as intersections.

(2) As the RBF-based method has good extrapolation capability, it is very suitable for constraint-based modeling of sparse drillhole data. Moreover, it is known that the orebody model usually has strong local continuity and extension trend along the direction of the mineralization area.

(3) Based on the anisotropy constraints, the anisotropic orebody model can be restrained by constructing geological trends in different directions according to the manual interpretation requirements of structural geologists.

References

[1] JESSELL M, AILLÈRES L, de KEMP E, LINDSAY M, WELLMANN F. Next generation three-dimensional geologic

modeling and inversion [J]. Economic Geology, 2014, 18: 261−272.
[2] COWAN J, BEATSON R, FRIGHT W R, MCLENNAN T J, MITCHELL T J. Rapid geological modeling [C]//Applied Structural Geology for Mineral Exploration and Mining International Symposium. Kalgoorlie: Australian Institute of Geologists, 2002: 23−25.
[3] COWAN E, SPRAGG K, EVERITT M. Wireframe-free geological modelling–An oxymoron or a value proposition [C]//Eighth International Mining Geology Conference. Melbourne: The Australasian Institute of Mining and Metallurgy, 2011: 247−260.
[4] MCLENNAN J A, DEUTSCH C V. Implicit boundary modeling (boundsim) [R]. Edmonton: University of Alberta, 2006.
[5] FRANK T, TERTOIS A L, MALLET J L. 3D-reconstruction of complex geological interfaces from irregularly distributed and noisy point data [J]. Computers & Geosciences, 2007, 33(7): 932−943.
[6] CUOMO S, GALLETTI A, GIUNTA G, MARCELLINO L. Reconstruction of implicit curves and surfaces via RBF interpolation [J]. Applied Numerical Mathematics, 2017, 116: 157−171.
[7] SKALA V. RBF Interpolation with CSRBF of large data sets [J]. Procedia Computer Science, 2017, 108: 2433−2437.
[8] MACÊDO I, GOIS J P, VELHO L. Hermite interpolation of implicit surfaces with radial basis functions[C]//Proceedings of 2009 XXII Brazilian Symposium on Computer Graphics and Image Processing. Rio de Janiero: IEEE, 2009: 1−8.
[9] FLEISHMAN S, COHEN-OR D, SILVA C T. Robust moving least-squares fitting with sharp features [J]. ACM Transactions on Graphics (TOG), 2005, 24(3): 544−552.
[10] BIRCH C. New systems for geological modelling-black box or best practice? [J]. Journal of the Southern African Institute of Mining and Metallurgy, 2014, 114(12): 993−1000.
[11] CARR J C, BEATSON R K, CHERRIE J B, MITCHELL T J, FRIGHT W R. Reconstruction and representation of 3D objects with radial basis functions [C]//Proceedings of the 28th Annual Conference on Computer Graphics and Interactive Techniques. New York: ACM, 2001: 67−76.
[12] COWAN E J, BEATSON R K, ROSS H J, FRIGHT W R, MCLENNAN T J. Practical implicit geological modeling [C]//Proceedings of Fifth International Mining Geology Conference. Victoria: Australian Institute of Mining and Metallurgy, 2003: 89−99.
[13] STOCH B, ANTHONISSEN C, MCCALL M, BASSON I J, DEACON J. 3D implicit modeling of the Sishen mine: New resolution of the geometry and origin of Fe mineralization [J]. Mineralium Deposita, 2018, 53(6): 835−853.
[14] JONES M W, CHEN M. A new approach to the construction of surfaces from contour data [J]. Computer Graphics Forum, 1994, 13(3): 75−84.
[15] GUO Jia-teng, WU Li-xin, ZHOU Wen-hui, LI Chao-lin, LI Feng-dan. Section-constrained local geological interface dynamic updating method based on the HRBF surface [J]. Journal of Structural Geology, 2018, 107: 64−72.
[16] CASCIOLA G, LAZZARO D, MONTEFUSCO L B, MORIGI S. Shape preserving surface reconstruction using locally anisotropic radial basis function interpolants [J]. Computers & Mathematics with Applications, 2006, 51(8): 1185−1198.
[17] CASCIOLA G, MONTEFUSCO L B, MORIGI S. Edge-driven image interpolation using adaptive anisotropic radial basis functions [J]. Journal of Mathematical Imaging and Vision, 2010, 36(2): 125−139.
[18] HILLIER M J, SCHETSELAAR E M, de KEMP E A, PERRON G. Three-dimensional modelling of geological surfaces using generalized interpolation with radial basis functions [J]. Mathematical Geosciences, 2014, 46(8): 931−953.
[19] ETTL S, KAMINSKI J, HÄUSLER G. Generalized Hermite interpolation with radial basis functions considering only gradient data [C]//Curve and Surface Fitting: Avignon 2006. Avignon: Nashboo Press, 2007: 141−149.
[20] GOIS J P, TREVISAN D F, BATAGELO H C, MACÊDO I. Generalized Hermitian radial basis functions implicits from polygonal mesh constraints [J]. The Visual Computer, 2013, 29(6−8): 651−661.
[21] FASSHAUER G E. Meshfree approximation methods with MATLAB [M]. London: World Scientific, 2007.
[22] WENDLAND H. Scattered data approximation [M]. Cambridge: Cambridge University Press, 2004.
[23] ZHONG De-yun, WANG Li-guan, JIA Ming-tao, ZHANG Ju. Orebody modeling from non-parallel cross sections with geometry constraints [J]. Minerals, 2019, 9(4): 1−17.
[24] HECKEL F, KONRAD O, HAHN H K, PEITGEN H O. Interactive 3D medical image segmentation with energy-minimizing implicit functions [J]. Computers & Graphics, 2011, 35(2): 275−287.
[25] SAAD Y, SCHULTZ M H. GMRES: A generalized minimal residual algorithm for solving nonsymmetric linear systems [J]. Siam Journal on Scientific & Statistical Computing, 1986, 7(3): 856−869.
[26] NIELSON G M, HAMANN B. The asymptotic decider: resolving the ambiguity in marching cubes [C]//Proceeding Visualization '91. California: IEE, 1991: 83−91.

融合地质规则约束的复杂矿体隐式建模方法

钟德云，王李管，毕 林，贾明涛

中南大学 资源与安全工程学院，长沙 410083

摘 要：为了根据结构地质学家的经验对矿体形状进行动态控制，基于广义径向基函数插值方法提出一种可以直接从原始钻孔数据进行矿体隐式建模的方法。发展多种约束规则来动态控制地质趋势，包括地质趋势线、地质约束线、地质趋势面、地质约束面和各向异性等，均可以转化为插值约束条件。结合约束规则的交互工具，该方法可以避免基于轮廓线拼接的显式建模方法存在的模型质量差、难以动态更新等缺点，对具有几何边界约束的矿体结构模型进行建模，简化矿体建模过程。数值试验结果表明，该隐式建模方法可以快速、准确、动态地建立三维矿体模型。

关键词：三维地质建模；隐式建模；径向基函数；结构各向异性；地质规则

(Edited by Xiang-qun LI)